Journal of Chromatography A 1731 (2024) 465154

Contents lists available at ScienceDirect

Journal of Chromatography A

journal homepage: www.elsevier.com/locate/chroma

Study of oxidation products in aged olive oils by GC and HPLC techniques coupled to mass spectrometry to discriminate olive oil lipid substances in archaeological artifacts from ancient Taormina (Italy)

Valentina Chiaia [a], Giuseppe Micalizzi [a,*], Danilo Donnarumma [a], Anna Irto [b], Clemente Bretti [b], Marta Venuti [c], Gabriele Lando [b], Luigi Mondello [a,d], Paola Cardiano [b]

[a] MeIT c/o Department of Chemical, Biological, Pharmaceutical and Environmental Sciences, former Veterinary School, University of Messina, Viale G. Palatucci snc 98168, Messina, Italy
[b] Department of Chemical, Biological, Pharmaceutical and Environmental Sciences, University of Messina, Viale Ferdinando Stagno d'Alcontres, 31 98166, Messina, Italy
[c] Department of Ancient and Modern Civilizations, University of Messina, Viale G. Palatucci snc 98168, Messina, Italy
[d] Chromaleont s.r.l., c/o Department of Chemical, Biological, Pharmaceutical and Environmental Sciences, University of Messina, Viale G. Palatucci snc 98168, Messina, Italy

ARTICLE INFO

Keywords:
Aged lipids
Archaeological markers
Pottery
Archaeometry
Chromatography-mass spectrometry

ABSTRACT

The identification of archaeological biomarkers is one of the main objectives of analytical chemistry in the archaeological field. However, no information is currently available on biomarkers able to unambiguously indicate the presence of olive oil, a cornerstone of Mediterranean ancient societies lifestyle, in an organic residue. This study aims to bridge this gap by a thorough characterization of the degradation products of extra-virgin olive oils (EVOOs) resulting from in-lab thermal oxidative treatments, with the primary goal of revealing potential archaeological biomarkers for olive oil. Thirty-three EVOOs sourced from eleven different monocultivars across five Italian regions (Sicily, Apulia, Lazio, Tuscany, and Liguria) and Spain, were analyzed before and after thermal oxidation. In addition, an identical thermal treatment was employed on pure triglyceride standards (triolein, trilinolein, and tristearin), due to the high concentration of their fatty acids in EVOO discerning their degradation patterns. A combination of analytical strategies was employed, including HPLC-MS and HPLC-ELSD for the complete evaluation of the intact lipids (triglycerides, diglycerides, and their oxidative species) in olive oils before and after oxidation, and HS-SPME-GC–MS and GC-FID for the characterization of secondary oxidation products formed by the thermal treatment. In addition, to elucidate the fatty acid distribution in the oxidized EVOOs by GC–MS and GC-FID techniques a derivatization step was performed to convert lipid compounds into trimethylsilyl (TMS) derivatives. A chemometric approach was used to thoroughly interpret the data obtained from intact and oxidized samples. This comprehensive investigation sheds light on the chemical transformations of EVOOs under thermal oxidative conditions and indicates mono-carboxylic acids such as pentanoic, hexanoic, heptanoic, octanoic, nonanoic, and decanoic acids as potential archaeological biomarkers for the presence of lipid substances coming from olive oil in archaeological organic residues. Finally, lipid contents from twenty-four real archaeological samples, grouped in *amphorae* (10), *unguentaria* (5), and *lamps* (9), excavated from the Roman *domus* of *Villa San Pancrazio* in Taormina (Italy), were determined. The analytical results obtained from *amphorae* samples revealed the presence of the selected olive oil-specific archaeological biomarkers, an information extremely interesting considering that this type of *amphorae* have so far been solely associated with the storage of wine.

* Corresponding author at: MeIT c/o Department of Chemical, Biological, Pharmaceutical and Environmental Sciences, former Veterinary School, University of Messina, Viale G. Palatucci snc 98168 – Messina, Italy.
E-mail address: giumicalizzi@unime.it (G. Micalizzi).

https://doi.org/10.1016/j.chroma.2024.465154
Received 25 May 2024; Received in revised form 5 July 2024; Accepted 8 July 2024
Available online 18 July 2024

1. Introduction

In archaeometry, analytical chemistry has dedicated significant attention to the investigation of organic matter preserved in the form of residues, surface deposits or encrustations within archaeological pottery. Considerable interest has been placed on studying lipids [1-3], due to their persistence in archaeological sites [4], since their hydrophobic nature limits percolation making them highly durable over time. However, the presence of reactive functional groups along their molecular structures may lead to their partial or complete degradation through chemical and microbiological processes such as hydrolysis and oxidation reactions in burial environments, which complicates the assessment the lipid matter origin [5]. Nevertheless, some favorable conditions can facilitate lipids preservation within pottery. Factors such as dry climatic conditions [6] and the nature of the organic or mineral materials in which lipids are encapsulated play a key role in their preservation. Lipids result also well-preserved in carbonized organic residues found on pottery [7].

In this context, the concept of *archaeological biomarker* [3] was introduced with the aim of identifying selective target molecules capable of providing highly predictive information about the origin of preserved organic residues. This, in turn, aids in establishing the function of ceramic vessels in which these residues are found [8]. Therefore, revealing the chemical nature of an archaeological biomarker stands as one of the main objectives of analytical chemistry in archaeological field [3]. For this purpose, artificial ageing studies mimicking natural decay processes over time of animal fats [9] and vegetable oils [10] have been carried out. Such experiments involve chemical degradation reactions such as thermal decomposition, oxidation, hydrolysis, and rearrangement followed by gas and/or liquid chromatography-mass spectrometry analyses to separate and identify the degradation products. For example, Colombini et al. [10] performed accelerated ageing experiments by thermo-oxidative treatments to induce degradation processes of a *Brassicaceae* seed oil (*Brassica juncea*), commonly employed in antiquity for lighting purposes. Gas chromatography-mass spectrometry (GC–MS) analyses allowed to establish the identity of degradation products and to reveal the archaeological biomarker useful for the probable identification of *Brassicaceae* seed oil in preserved organic residues. Similarly, lipids contained in organic residues were distinguished into aquatic or terrestrial kingdoms based on the carbon chain length of ω-(o-alkylphenyl) alkanoic acids (APAAs) [9]. Consequently, APAAs containing 20 or 22 carbon atoms could potentially be related to their precursor eicosapentaenoic (C20:5n3) and docosahexaenoic (C22:6n3) acids, prevalent in aquatic organisms. Conversely, APAAs with 16 and 18 carbons reflect the molecular structures of lipids originating from terrestrial kingdom, including animals and plants.

As far as the authors are aware, there is currently no available information regarding archaeological biomarkers that could specifically indicate the presence of lipid substances derived from olive oil in archaeological organic residues. The archaeological significance of olive oil is underscored by textual sources, which highlight its prominence as one of the most used commodities in ancient societies. Literary sources and some scholars also suggest a conspicuous production of olive oil in the hinterland of ancient Taormina, for which it is possible to hypothesize that several containers found with excavations were designed for the storage and commercialization of olive oil. Simultaneously, a long tradition of *amphorae* production is archaeologically attested, starting from the Hellenistic period (MGSIII type, Dressel 1 type), continuing through the imperial age (Dressel 2/4 type, Spinella type), and extending into late antiquity (Keay LII type). Also, several kilns have been investigated in the area of Giardini Naxos (Italy), unequivocally clarifying the presence of a thriving economy centered on agricultural products within these *amphorae* [11,12]. So far, these types of *amphorae* have only been associated with the marketing of the well-known "*vino tauromenitano*". However, from an archaeological perspective, the study of *amphorae* does not provide decisive information. Both the Spinella type and Keay LII type are morphologically standardized artifacts, and there has been no technological difference observed, such as the presence of special internal coatings like pitch or resin designed to waterproof the surfaces. Additionally, further data includes the discovery of several factories in the *chora* of *Tauromenion*, typologically related to both wine and oil production [13]. A long tradition of studies has shown that the economy of *Tauromenion* was based on sheep farming, and the production of oil and wine starting from the Hellenistic period [13].

This research attempt to fully characterize the decay products in extra-virgin olive oils (EVOOs) induced by in-lab thermal oxidative treatments, with the aim of revealing specific archaeological biomarkers that could provide insight about the employment of *amphorae* for olive oil storage. Since lipid distribution is significantly influenced by the olive variety and the geographical origin [14], thirty-three EVOOs belonging to different monocultivar varieties and coming from several Italian regions and Spain were subjected to ageing experiments and following analyses. The identity of triglycerides (TAGs), diglycerides (DAGs), and their oxidized species was established by means of high-performance liquid chromatography-mass spectrometry (HPLC-MS), while the quantitative profiling of TAGs in original EVOOs was determined using a liquid chromatograph coupled to evaporative light scattering detector (HPLC-ELSD). Also, thermal oxidation process induced the formation of a wide variety of secondary products of oxidation including carboxylic acids, alcohols, hydrocarbons, esters, ketones, lactones, aldehydes, and furans. Head-space solid phase microextraction (HS-SPME) technique coupled with gas chromatography-mass spectrometry (GC–MS) and gas chromatography-flame ionization detection (GC-FID) was employed for the analyses of these volatile substances. Further, all the lipid substances including mono- and dicarboxylic acids, and monoglycerides (MAGs) were derivatized into trimethylsilyl ether (TMS) derivatives by using a silylating reagent and detected by GC–MS and GC-FID. In order to assess the degradation patterns in olive oils, thermal oxidation treatment was also carried out for pure TAG standards consisting in triolein (OOO), trilinolein (LLL), and tristearin (SSS), according to the predominant distribution of their fatty acids in EVOO. Multivariate statistical analyses were employed to elucidate decay patterns in olive oils and to identify potential chemical compounds serving as archaeological biomarkers to indicate the presence of olive oil in organic residues. The study indicated pentanoic, hexanoic, heptanoic, octanoic, nonanoic, and decanoic acids as specific archaeological biomarkers for the presence of lipid substances coming from olive oil in organic residues found in archaeological context. This research also comprise the analysis of organic residues extracted from Hellenistic and Roman pottery, as well as the ones recovered from encrustations or soil found within ceramic vessels excavated at the archaeological site of the *domus* of *Villa San Pancrazio* in Taormina (Italy).

2. Materials and methods

2.1. Standards and chemicals

All solvents used in this research work were supplied by Merck Life Science (Darmstadt, Germany). Specifically, chloroform (HPLC, ≥99.8%), methanol (hypergrade for LC-MS LiChrosolv®), dichloromethane (HPLC, ≥99.8%), isopropanol (gradient HPLC grade, *ca.*99.8%), and acetonitrile (gradient grade for liquid chromatography) were employed. For the conversion of the volatile lipids into TMS derivatives, N,O-bis(trimethylsilyl)trifluoroacetamide (BSTFA) reagent containing 1% of trimethylchlorosilane (Merck Life Science) was utilized. A reference standard solution of carbon saturated C7–C40 alkanes (Merck Life Science) was used for the determination of the linear retention index (LRI) in GC–MS analyses. In addition, a mixture of odd carbon number TAGs ranging from trinonanoin ($C_9C_9C_9$) to triheptadecanoin ($C_{17}C_{17}C_{17}$) was used as a reference homologue series (single TAGs were purchased from Merck Life Science) for determining the LRIs

in HPLC-MS analyses.

2.2. In-lab ageing experiments of olive oils and pure TAG standards

A total of thirty-three EVOOs sourced from various monocultivars and regions in Italy and Spain were purchased for this study. The geographical origin and monovarietal olive oils were as follows: Sicily, nocellara del Belice (3) and biancolilla (3); Apulia, ogliarola (3) and coratina (3); Lazio, caninese (3) and frantoio (3); Tuscany, leccina (3) and frantoio (3); Liguria, taggiasca (3); Spain, hojiblanca (2), picual (2), and arbequina (2). For each olive oil sample, 10 mg were transferred in a 4 mL glass vial with cap and thermically oxidized in an oven at 120 °C for three weeks [10]. TAG standards including tristearin (purity ≥ 99%), triolein (purity ≥ 99 %), and trilinolein (purity ≥ 98 % TLC) were acquired from Merck Life Science. Subsequently, 10 mg of each standard were weighted and transferred in a 4 mL glass vial with cap for ageing treatment, following the procedure described above.

2.3. HPLC-MS and HPLC-ELSD analyses of lipids

10 mg of olive oil, before and after thermal oxidation process, were diluted in 1 mL of isopropanol (final concentration 10,000 mg L^{-1}). The separation and identification of lipids in EVOOs were carried out as reported in Oteri et al. [14], with minor modifications. For details refer to the Supplementary material. For LRI calculation, the odd carbon number TAG mixture was used as reference homologue series [14]. A lab-constructed database containing LRI values was utilized as reference. TAGs composition in the not-aged EVOOs was investigated following the method outlined in Rigano et al. [15]. A detailed description of the analytical specifications is reported in Supplementary material. Each sample was analyzed in triplicate.

2.4. HS-SPME-GC–MS and GC-FID analyses of secondary oxidation products in thermal oxidized samples

HS-SPME analyses of the secondary oxidation products in aged samples were carried out by using a SPME fiber coated with divinylbenzene/carboxen/polydimethylsiloxane (DVB/CAR/PDMS) phases (Merck Life Science). SPME fiber specifications are as follows: 30 μm d_f CAR/PDMS layer, 50 μm d_f DVB layer, 2 cm long, needle size 24 ga. The HS-SPME protocol consisted of an initial sample conditioning time of 15 min at 70 °C, followed by fiber exposure in the vial headspace containing thermically oxidized samples (olive oil and TAG standards); exposure time was of 30 min at 70 °C, stirring rate of 300 rpm. Finally, the analytes were thermically desorbed for 1 min at 250 °C in the injection port of the gas chromatograph.

GC–MS analyses were performed on a GCMS-QP2020 NX system (Shimadzu) equipped with a split/splitless injector (250 °C) and an inlet liner, direct (SPME) type, straight-through design (unpacked) (Shimadzu) of dimensions 95 mm × 5.0 mm OD × 0.75 mm ID (liner volume 40 μL). The separation of analytes was achieved by using a RTX-1301 (Restek) capillary column, 30 m x 0.25 mm ID x 0.25 μm d_f. Helium was used as carrier gas at a constant linear velocity of 30 cm sec^{-1} and a pressure of 26.7 kPa. Samples were injected in splitless mode (1 min of sampling time). The chromatographic separation was performed according to the following temperature program: 40 °C (1 min) to 280 °C at 2 °C min^{-1}. MS parameters were as follows: electron ionization, 70-eV; ion source temperature, 250 °C; mass range, m/z 40–650; interface temperature, 250 °C. A C_7—C_{30} saturated alkanes standard mixture was used for LRI calculation. In such a respect, two different criteria were employed for the identification of compounds: mass spectral similarity and LRI correspondence. The GCMS Solution software (version 4.50 Shimadzu) was used for both data acquisition and processing.

GC-FID analyses were carried out on a gas chromatograph Nexis GC-2030 (Shimadzu) coupled to FID detector. The instrument was equipped with a split/splitless injector (250 °C) and an inlet liner, direct (SPME) type. The capillary column, temperature program, and gas linear velocity were the same as described for GC–MS analysis, except for the inlet pressure 99.4 kPa. FID temperature was set at 260 °C (sampling rate 40 ms); gas flows were 40 mL min^{-1} for hydrogen, 10 mL min^{-1} for make-up gas (nitrogen) and 400 mL min^{-1} for air. Data were acquired and processed through LabSolutions software (vers. 5.92, Shimadzu).

2.5. Silylation and GC–MS and GC-FID analyses of lipids in thermal oxidized samples

For the silylation protocol, 200 μL of N,O-Bis(trimethylsilyl) trifluoroacetamide (BSTFA) reagent containing the 1% of trimethylchlorosilane (TMCS) and 500 μL of dichloromethane were employed. The derivatization temperature was maintained at 80 °C for 20 min. The dichloromethane phase containing TMS derivatives was collected, transferred to glass autosampler vial, and injected into GC–MS and GC-FID systems. GC–MS and GC-FID analyses of TMS derivatives were performed as described in Zheljazkov et al. [16]. Details are reported in Supplementary materials. All samples were analyzed in triplicate for a major data precision.

2.6. Statistical analysis

All chemometric treatments were carried out using MATLAB (R2021a version, The Mathworks Inc. Natik, MA) and PLS_Toolbox (version 8.7, Eigenvector Research Inc., Wenatchee, WA). Principal component analysis (PCA) was employed to reveal patterns in the samples and as untargeted tool for identifying potential chemical compounds that could serve as archaeological biomarkers for the presence of olive oil in lipid matter preserved in ancient samples. A total of 33 olive oil samples were analyzed for the quantitative determination, expressed in relative concentration (area normalization), of 8 TAGs before ageing (HPLC-ELSD, 8 variables) and of 49 volatile lipids after ageing (GC-FID, 49 variables). The GC-FID and HPLC-ELSD datasets were analyzed separately after column autoscaling to check for differences among samples before and after ageing.

2.7. Archaeological samples and GC–MS analyses

The selected materials came from the excavations of the Roman *domus* of Taormina, specifically from the area of *Villa San Pancrazio* [17-19]. These excavations yielded significant remains associated with four *domus* dating between the 1st and 2nd centuries AD. In the case of *Domus* 2, artifacts useful for reconstructing the ceramic sets used within the *domus* were discovered.

It has been chosen to analyze and compare samples from artifacts belonging to functional categories which, from what is known from literary sources, are connected to the use of olive oil: *amphorae* (10 samples) used for food transport and storage; *unguentaria* (5 samples) used to contain oils and perfumes; *lamps* (9 samples) utilized for household lighting. The list of the analyzed samples and their specifications is reported in Table 1. These have been selected according to a series of requirements that concern both the artifacts and the context of deposition in the stratigraphic sequence. The selected artifacts come from stratigraphic units with a high degree of reliability, not subject to alteration phenomena, natural or anthropic, and therefore preserved in their original condition of deposition (primary deposition). Furthermore, the degree of preservation of individual artifacts was also evaluated, preferring those that were better preserved and could provide greater assurance of preserving their original content within them. In the case of *lamps* and *unguentaria* this criterion has always been respected: the size of the artifacts and their nature generally favor their preservation in the record. On the contrary, in the case of *amphorae,* which are larger artifacts subject to different processes of destruction, it was not possible to take samples from an intact one in any case.

The artifacts, recovered from archaeological layers with an earthy

Table 1
List of archaeological samples classified according to the function of the original ceramic vessel in ancient time, and type of sample.

Sample Code	Function of artifact	Type of sample	Note
8041–1	Amphora	Pottery	Keay LII type-IV-VI cent. AD
US3329 RO 8	Amphora	Soil	Spinella type-I cent. AD
US3329 RO 11	Amphora	Soil	Spinella type-I cent. AD
US3329 RO 19	Amphora	Soil	Spinella type-I cent. AD
US3329 RO 21	Amphora	Soil	Spinella type-I cent. AD
US3329 RO 23	Amphora	Pottery	Spinella type-I cent. AD
US3329 RO 24	Amphora	Pottery	Spinella type-I cent. AD
US3329 RO 25	Amphora	Pottery	Spinella type-I cent. AD
US3329 RO 26	Amphora	Soil	Spinella type-I cent. AD
US3329 RO 28	Amphora	Pottery	Spinella type-I cent. AD
2075–1A	Unguentarium	Pottery	Small achroma jug II-I cent. BC
2075–1B	Unguentarium	Encrustation	Small achroma jug II-I cent. BC
2080–2B	Unguentarium	Soil	Black gloss lekythos III-II cent. BC
2052–1	Unguentarium	Pottery	Small achroma jug II-I cent. BC
2062–1	Unguentarium	Soil	Small achroma jug II-I cent. BC
2029–3	Lamp	Soil	Red gloss lamp I cent. BC/ I cent. AD
2080–5	Lamp	Soil	Black gloss lamp II-I cent. BC
2029–2	Lamp	Soil	Achroma lamp II-I cent. BC
2052–3	Lamp	Soil	Achroma lamp II-I cent. BC
2088–1A	Lamp	Soil	Red gloss lamp I cent. BC/ I cent. AD
2088–1B	Lamp	Soil	Red gloss lamp I cent. BC/ I cent. AD
2080–1	Lamp	Soil	Achroma lamp II-I cent. BC
2077–1	Lamp	Soil	Red gloss lamp I cent. BC/ I cent. AD
2029–1	Lamp	Soil	Achroma lamp II-I cent. BC

matrix, were stored inside aluminum paper wrappers until sampling. Visible residues, whenever present, were collected using a sterile metal blade. The extraction of the lipid content from ceramic archaeological samples followed a reported procedure: 2 g of ground pottery was extracted using a volume of 7.5 mL of a chloroform/methanol mixture (2:1 v/v) [20]. To enhance lipid extraction, the samples were sonicated for 15 min at room temperature. Subsequently, the extraction mixture was centrifuged at 3000 rpm for 15 min to deposit the remaining fine particles. The liquid fraction was recovered and dried using an EZ-2 Personal-Evaporator (Genevac). All lipid substances were derivatized using 50 μL of BSTFA reagent containing the 1% of TMCS and 150 μL of dichloromethane; derivatization temperature: 80 °C for 20 min. The dichloromethane phase containing TMS derivatives was collected, transferred to glass autosampler vial, and injected into GC–MS system.

GC–MS analyses of TMS derivatives were performed according to the analytical conditions previously described in paragraph 2.5, except for the injection volume (2 μL in splitless mode).

3. Results and discussion

The primary objective of this study is to comprehensively characterize the oxidation products induced by in-lab thermal treatments in olive oil, aiming to identify potential specific archaeological biomarkers in ancient organic residues. Previous researches have demonstrated significant variability in lipids distribution among olive oils from different monocultivars and geographical origins [14,21,22]. Pedoclimatic conditions and cultivars are known to influence the lipid distribution in olive oils. However, the impact of these variables on the formation of degradation products induced by thermal oxidation processes remains unclear. Thus, thirty-three EVOOs belonging to eleven different monocultivars sourced from five Italian regions and Spain, were analyzed before and after thermal oxidation process at 120 °C for three weeks. Identical treatment was also applied to pure triglyceride standards such as OOO, LLL, and SSS to assess degradation patterns in olive oils.

3.1. Lipids profiling by HPLC-MS

A NARP-HPLC-APCI-MS method was applied for evaluating the oxidation grade of lipids in oxidized olive oils. The elution order of the lipid species depends on their partition number (PN), derived from the equation PN = CN − 2DB, where CN and DB are the carbon number and double bond number of FAs in the structure, respectively. The identification was carried out according to Oteri et al. [14], by using two different identification criteria: MS fragment patterns and LRIs. The list of the identified lipid species is reported in Table 2 as well as their retention times (RT), diagnostic fragments, PN, experimental and reference LRIs. HPLC-MS chromatograms of the EVOO sample cultivar “biancolilla”, before and after thermo-oxidative treatment, are shown in Fig. 1.

The upper chromatogram (A) illustrates the typical profile of TAGs in olive oil. A total of 13 TAGs (PNs ranging from 42 to 50) were revealed with OOO, POO, OOL, and POL as main components. Oxidation in air at 120 °C extended for three weeks caused the formation of oxidized lipids, both DAGs and TAGs (Fig. 1-B), such as mono-hydroxy forms (*e.g., Ox*-OO or *Ox*-OOO) characterized by a mass increase of 16 Dalton respect to the not-oxidized lipid parent, and bis-hydroxy species (*e.g.*, 2 *Ox*-OOO) with an increasing of 32 Dalton (see Table 2). Interestingly, all the oxidized species, except for the very low abundant *Ox*.OLP compound, contain oleic acid as the only unsaturated fatty acid, strongly indicating this compound as the main target of the oxidation process in olive oil. It is generally accepted that the process of formation of oxidized lipids proceeds by hydroperoxides, the primary products of oxidation, and it involves a free radical mechanism that includes the reaction between an allylic hydrogen (H) and peroxyl radical (O_2) [23]. The higher susceptibility of unsaturated acyl chains to thermal oxidation than saturated isologous acyl chain is dependent on the availability of allylic hydrogen. The abstraction of the hydrogen on the carbon atom close to double bond determines the formation of allylic radicals characterized by a high stability (electrons result delocalized on three carbon atoms) [23]. Resonance structures of the allylic system generate a series of hydroperoxide isomers. For example, the autoxidation of the oleic acid determines the formation of four isomers as follows: 8-hydroperoxide-9-octadecenoic acid, 11-hydroperoxide-9-octadecenoic acid, 10-hydroperoxide-8-octadecenoic acid, and 9-hydroperoxide-10-octadecenoic acid. For linoleic acid, the abstraction of the allylic hydrogen is favoured at C11 position because it leads to the formation of the very stable pentadienyl radical in which the electrons result delocalized on five carbon atoms [23]. The attack of peroxyl radical occurs mainly on C9 and C13 positions in equal manner with formation of two isomers as principal hydroperoxides: 13-hydroperoxide-9,11-octadecadienoic acid and 9-hydroperoxide-10,12-octadecadienoic acid [23]. A homolytic cleavage of the oxygen-oxygen bond causes the formation of the alkoxy radical (-O˙), which after reaction with

Table 2
Lipid species identified in olive oils before and after thermal oxidation process. Abbreviations: RT: retention time; $[M\text{-}H_2O+H]^+$, $[M+H]^+$, $[M+NH_4]^+$ and diagnostic fragments: detected ions; Class: lipid class; CN: DB: carbon number: double bond; PN: partition number; LRI_{exp}: experimental LRI; LRI_{ref}: reference LRI [14].

Compound	RT	$[M\text{-}H_2O+H]^+$	$[M+H]^+$	$[M+NH_4]^+$	Diagnostic Fragments	Class	CN:DB	PN	LRI_{exp}	LRI_{ref}
Ox. PO	2.967	593.5	611.5	–	313.3–355.3	*Ox.* DAG	34:1	32	2844	–
Ox. OO	2.967	619.5	637.5	–	339.3–355.3	*Ox.* DAG	36:2	32	2865	–
PO	6.503	577.5	–	–	313.3–339.3	DAG	34:1	32	3327	–
OO	6.503	603.5	–	–	339.3	DAG	36:2	32	3327	–
2 *Ox.* OOO	14.321	–	–	–	635.5	*2Ox.* TAG	54:3	48	3827	–
Ox. POL	20.033	–	873.7	890.8	591.5–593.5–617.5	*Ox.* TAG	52:3	46	4178	–
Ox. POO	22.522	–	875.7	–	593.5–619.5	*Ox.* TAG	52:2	48	4249	–
OLLn	22.743		879.7	896.7	597.5–599.5–601.5	TAG	54:6	42	4252	4192
Ox. OOO	23.081	–	901.7	–	619.5	*Ox.* TAG	54:3	48	4265	–
Ox. PPO	23.860	–	849.7	–	593.5	*Ox.* TAG	50:1	48	4288	–
OLL	26.175		881.7	898.7	599.5–601.5	TAG	54:5	44	4348	4342
PLL	26.582		855.7	872.7	575.5–599.5	TAG	52:4	44	4366	4358
POLn	27.013		855.7	872.7	573.5–577.5–599.5	TAG	52:4	44	4385	4383
Ox. SOO	27.315	–	–	920.9	621.6–619.5	*Ox.* TAG	54:2	50	4474	–
Ox. PSO	27.711	–	–	894.8	621.6–619.5–593.2	*Ox.* TAG	52:1	50	4493	–
OOL	29.525	–	883.7	900.7	601.5–603.5	TAG	54:4	46	4528	4516
POL	29.805	–	857.7	874.8	575.5–577.5–601.5	TAG	52:3	46	4551	4539
PPL	30.875		831.7	848.7	551.4–575.4	TAG	50:2	46	4574	4571
OOO	32.445	–	885.7	902.9	603.5	TAG	54:3	48	4722	4729
POO	32.829	–	859.7	876.8	603.5–577.5	TAG	52:2	48	4749	4756
PPO	33.330	–	–	850.8	551.5–577.5	TAG	50:1	48	4777	4776
PPP	33.911	–	–	824.8	551.5	TAG	48:0	48	4811	4799
SOO	36.645	–	887.7	904.9	603.5–605.5	TAG	54:2	50	4945	4948
PSO	37.145	–	–	878.9	579.5–605.6–577.5	TAG	52:1	50	4977	4961
OOG	37.529		913.8	930.8	603.5–631.5	TAG	56:3	50	4997	4905
PPS	37.576	–	–	852.8	551.4–605.6	TAG	50:0	50	4999	4978

Note: *Ox.* DAG: oxidized diglyceride; DAG: diglyceride; *Ox.* TAG: oxidized triglyceride; TAG: triglyceride. Abbreviations: P: palmitic acid (C16:0); S: stearic acid (C18:0); O: oleic acid (C18:1n9); L: linoleic acid (C18:2n6); Ln: α-linolenic acid (C18:3n3); G: gadoleic acid (C20:1n9).

hydrogen free radical (-H), forms the hydroxy species detected in HPLC-MS analysis. However, the alkoxy radicals can also react to form secondary products of oxidation such as volatiles, especially when they are exposed to oxidation conditions as heat for extended periods [24]. The mechanism of reaction involves a carbon-carbon cleavage, which can occur on either side of the alkoxy radical group with formation of a carbonyl group. Their monitoring will be discussed later.

3.2. TAGs composition of the not-aged EVOOs by HPLC-ELSD

The separation and quantification of triglycerides in the thirty-three EVOO samples, before thermo-oxidative treatment, were performed in accordance with Rigano et al. [15]. The use of two serially coupled C18 columns allowed the separation of the more abundant TAGs with an optimal resolution in accordance with their PNs. TAGs composition of the EVOOs expressed in terms of percentage area ± standard deviation (SD) is reported in Table S1. Principal component analysis of the HPLC-ELSD data revealed that the olive oils exhibited different patterns in terms of relative abundance of TAGs. This behavior, already reported by Oteri et al. [14], is illustrated in Fig. 2-A. The score plot in the PC1 *vs* PC2 space showed that samples from different regions were distinctly separated. As an example, Apulia samples consistently displayed low values on PC1 and were grouped near zero on PC2. Liguria samples, in contrast, had positive values on PC1, with relatively low variability in their pattern (*i.e.*, size of the polygon). This can be attributed to the fact that Ligurian samples came from a single cultivar, whereas samples from other regions are from at least two different cultivars. The Spanish samples exhibited greater variability, likely due to the vast geographic region they represented. The loading in Fig. 2-B indicated that PC1 primarily accounted for the variance associated with unsaturated TAGs, particularly OOO (negative values on PC1, −0.45) and TAGs containing linoleic acid (positive values on PC1: OLO = 0.45, OLL = 0.45, OLP = 0.45). On the other hand, PC2 explained the variance related to the presence of saturated fatty acid, such as palmitic (negative values on PC2, OOP+POP = −0.55) and stearic acid (positive values on PC2, SOO = 0.6, SOP = 0.35).

3.3. Secondary oxidation products by HS-SPME-GC–MS and GC-FID analyses

The characterization of secondary oxidation products formed by in-lab thermal treatment at 120 °C extended for three weeks was carried out by using HS-SPME-GC–MS and GC-FID techniques. The overall results show the formation of several oxidized species grouped in eight classes of chemical compounds including carboxylic acids, esters, alcohols, hydrocarbons, ketones, aldehydes, lactones, and furans. For a better understanding of the oxidation patterns, the same oxidative treatment was also applied to OOO, LLL, and SSS triglycerides in accordance with the predominant distribution of their fatty acids in olive oil. A total of 119 oxidized volatiles (see Table S.2) were identified and quantified (relative concentration) in the analyzed samples. Table 3 reports the composition of the volatiles identified in the oxidized samples, grouped in compounds classes.

As previously described, the different susceptibility of TAGs to thermal oxidation depends on the availability of allylic hydrogen. This means that saturated fatty acids contribute partially to the formation of secondary oxidation products in accordance with literature data [25]. However, a partial oxidation occurred in SSS as reported in Table S2, but still less than corresponding unsaturated isologue triglycerides. Predominant decay products were aldehydes (29.78%) and hydrocarbons (29.58%) along with minor amounts of carboxylic acids (2.66%), and ketones (1.32%) plus about 19.41% of other compounds (benzothiazole, carbon disulfide and sulfur dioxide). Aldehydes included a homologous series of compounds ranging from acetaldehyde to decanal that originated sequentially from the parent fatty acid in stepwise degradation, losing one carbon atom per degradation step. Consequently, no specific oxidative attack occurred in SSS, but each methyl-portion in the fatty acyl chain appeared to be susceptible to thermal oxidation. With respect to hydrocarbons, the presence of such compounds among secondary oxidation products can be explained by the reaction of free alkyl radicals, induced by thermal oxidation, with free hydrogen radicals [23]. Almost all the compounds were grouped in methyl-branched aliphatic hydrocarbons, namely branched-C_{12}-, branched-C_{15}-, and

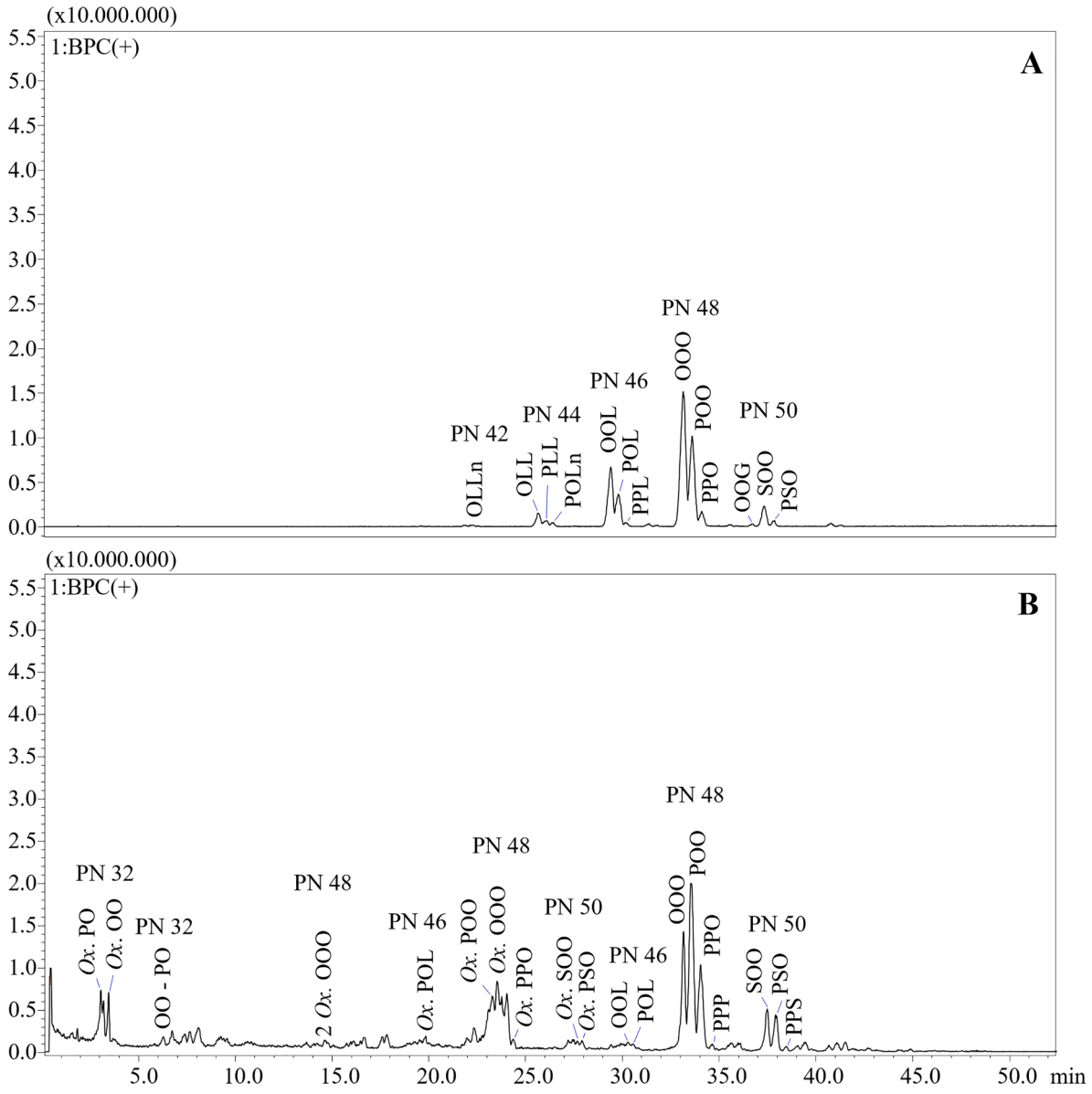

Fig. 1. HPLC-MS chromatograms of lipid species in olive oil cultivar "biancolilla", before (A) and after (B) thermal oxidation.

branched-C_{18}-alkanes. They were distinguished from the straight chain isomers by preferential fragmentation at the branch site resulting the formation of distinctive fragment ions. For instance, in the case of branched-C_{12}-alkanes, the prominent base peak at *m/z* 71, indicating the favored $C_5H_{11}^+$ fragment (stable secondary carbocation), and fragment ion at *m/z* 127, corresponding to the $C_9H_{19}^+$ fragment, suggested that a methyl group was located on the fourth carbon atom along the acyl chain. Further, the molecular ions at *m/z* 170 confirmed that these compounds were structural isomers of the dodecane (molecular weight 170 uma), thus they were grouped into branched-C_{12} alkanes. Differently, MS spectrum of the straight chain dodecane showed the base peak at *m/z* 57, corresponding to the $C_4H_9^+$ portion, and other smaller fragments separated by 14 units of *m/z* resulting from the loss of sequential CH_2 group. The intensity of the ions after 57 *m/z* decreased in exponential manner according to common trends of the straight chain alkanes [26]. Similar considerations regarded branched-C_{15}- (base peak at *m/z* 71, molecular ion at *m/z* 212) and branched-C_{18}- (base peak at *m/z* 71, molecular ion at *m/z* 254) alkane groups.

A total of 43 secondary oxidation products were determined in oxidized LLL triglyceride. Major volatiles included carboxylic acids with a relative abundance of 70.78%, with pentanoic (6.84%), hexanoic (36.88%), heptanoic (8.47%), and octanoic (8.06%) acids as preponderant decomposition products. The conspicuous amount of hexanoic acid reflected the double bond position at C6 of the linoleic acid counting from the terminal portion of the acyl chain, indicating a preferential oxidative attack under the experimental conditions. Therefore, hexanoic acid could be ascribed to oxidation processes of the linoleic acid and consequently considered as its probable biomarker. It should be noted that distribution patterns of carboxylic acids showed some similarities with the distribution patterns of aldehydes (pentanal 0.62%, hexanal 1.79%, heptanal 0.23%, and octanal 0.15% were the prominent aldehydes). These affinities indicate that various acids may form by oxidation of the corresponding carbon chain aldehydes. Furthermore, considering the formation mechanism of hexanal via hydroperoxide degradation [27], it can be assumed that 13-hydroperoxide-9,11-octadecadienoic acid was the most prominent isomer among those previously described. Among the volatiles, a series of γ- and δ-lactones were also identified. It was reported that the formation of these compounds is promoted by the reduction of hydroperoxides and carbon-carbon cleavage along the acyl chain in heated oils [28]. The

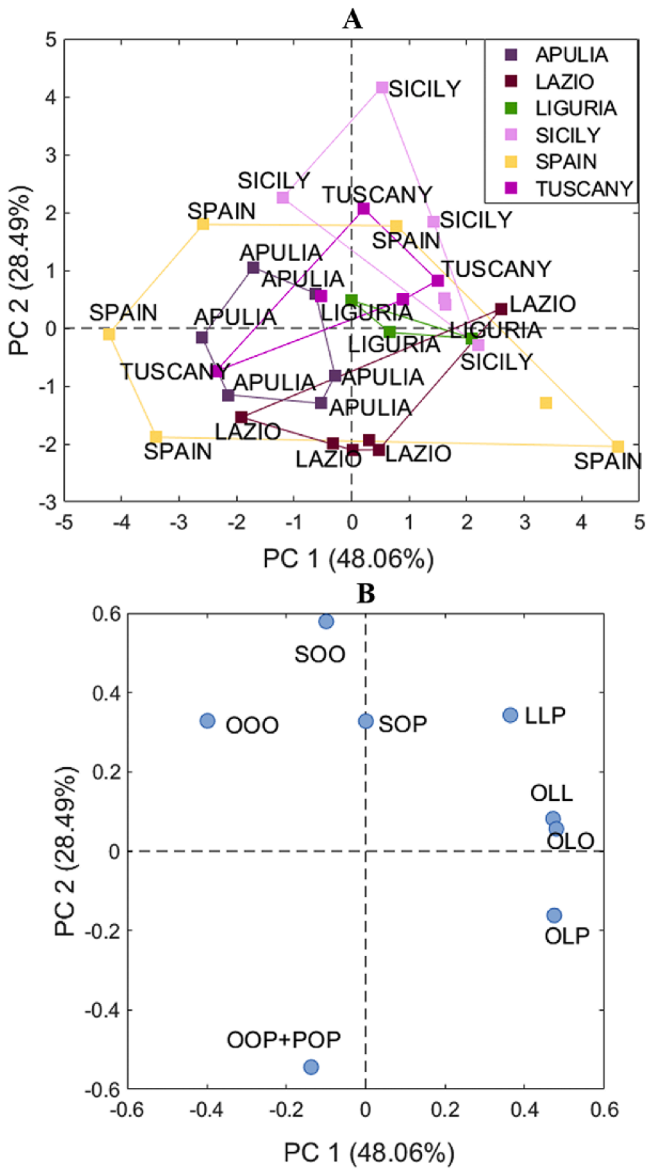

Fig. 2. Score (A) and loading (B) plots of the HPLC-ELSD data relative to the thirty-three not-aged EVOOs.

Table 3
Chemical classes of volatiles identified in tristearin (SSS), trilinolein (LLL), triolein (OOO), and olive oil cultivar "biancolilla". Quantitative data are expressed in relative percentage (%). Numbers in parentheses show the number of compounds in each chemical class.

Chemical Class	SSS	LLL	OOO	EVOO
Carboxylic Acids	(5) 2.66	(12) 70.78	(10) 55.37	(11) 43.32
Esters	(0) 0.00	(4) 1.25	(13) 7.29	(19) 6.97
Alcohols	(2) 0.85	(1) 0.06	(3) 0.39	(2) 0.20
Hydrocarbons	(18) 29.58	(0) 0.00	(9) 1.04	(17) 11.16
Ketones	(7) 1.32	(6) 2.06	(13) 8.06	(15) 9.84
Aldehydes	(9) 29.78	(8) 3.37	(9) 12.35	(13) 11.62
Lactones	(1) 0.13	(11) 7.70	(8) 9.13	(10) 7.44
Furans	(0) 0.00	(0) 0.00	(1) 0.19	(2) 1.01

mechanism of reaction also involves an intramolecular esterification (lactonization) when the hydroxyl group of a fatty acid is located near a carboxylic group. The location of the hydroxyl group on acyl chain determines the resulting γ- and δ-lactones [28]. A total of 11 lactones were present with γ-nonalactone (1.74%) as main component according to the double bond position at C9 in linoleic acid. However, it must also be reported a series of γ- and δ-lactones such as butyrolactone (0.17%), γ- (0.20%) and δ-pentalactones (0.76%), γ- (1.16%) and δ-hexalactones (0.70%), γ-heptalactone (0.42%), γ- (0.98%) and δ-octalactones (0.77%), γ-decalactone (0.25%), and finally massoia lactone (0.55%).

With respect to triolein, the high susceptibility to thermal oxidation was demonstrated from the high number of volatiles (67 compounds) identified. Carboxylic acids were the major chemical class with heptanoic (10.62%), octanoic (17.31%), and nonanoic (13.38%) acids as main components along with minor amounts of formic (4.80%), acetic (1.33%), propanoic (0.19%), butanoic (0.61%), pentanoic (1.69%), hexanoic (4.56%), and decanoic (0.88%) acids. The second class of volatiles in terms of abundance was represented by the aldehydes with heptanal (2.05%), octanal (3.04%), and nonanal (4.48%) as principal components. Their formation was probably the result of the decomposition of the main four isomers of hydroperoxide-9-octadecenoic acid. In addition, a series of minor aldehydes were also revealed such as propanal (0.01%), butanal (0.12%), pentanal (0.30%), hexanal (0.95%) and decanal (1.05%). As described above, such distribution patterns reflected the distribution patterns of carboxylic acids, endorsing the hypothesis previously described. Also, thermal treatment determined the formation of a homologous series of lactones (8 components) as shown in Table S2. A predominance of γ-lactones (butyrolactone 0.28%, γ-hexalactone 0.50%, γ-heptalactone 1.67%, γ-octalactone 2.69%, γ-nonalactone 2.83%, and γ-decalactone 0.25%) were found, while only two δ-lactones (δ-pentalactone 0.41% and δ-nonalactone 0.50%) were detected. It should be noted that a significant prevalence of lactones with seven, eight and nine carbon atoms were revealed; similar trend was also highlighted for carboxylic acid and aldehyde classes. A remarkable number of ketones (13 compounds) distributed mainly along a homologous series of methyl-ketones were also determined: propan-2-one (0.03%), pentan-2-one (0.02%), hexan-2-one (0.10%), heptan-2-one (0.29%), octan-2-one (0.89%), nonan-2-one (2.13%), decan-2-one (2.73%), and undecane-2-one (0.31%). Literature data indicate that unsaturated fatty acids are responsible for the formation of methyl-ketones, but their paths of formation are not completely elucidated [29]. Probably, their origin occurs by oxidation of unsaturated aldehydes with a double bond in C2 or C4 positions [29]. Finally, 13 ester compounds were also identified among secondary products of the oxidized triolein. Conventionally, esters are formed when carboxylic acids are heated in presence of alcohols, therefore their distribution can reflect the content of the carboxylic acids with the same acyl chain length. Nevertheless, considering the capability of the HS-SPME technique of sampling exclusively volatiles and semivolatiles with specific range of volatility (SPME fibre specifications: 40–275 uma), this trend was partially observed. Further insight into the ester distribution will be elucidated in the next section.

As illustrated in HS-SPME-GC-MS chromatograms of Fig. 3, oxidation patterns of triolein and olive oil showed evident similarities. Such behavior was not surprising considering the high abundance of OOO in olive oil. This means that degradation of individual lipid components can provide highly predictive information on degradation patterns of olive oils according to their distribution in fresh material.

As example, in-lab oxidation process of a representative EVOO ("biancolilla" cultivar) mainly resulted in the formation of carboxylic acids (43.32%), with pentanoic (2.86%), hexanoic (7.94%), heptanoic (5.44%), octanoic (9.24%), nonanoic (6.50%), and decanoic (0.26%) acids as main components. Focusing on pentanoic and heptanoic acids, their presence among secondary oxidation products can be ascribed to the simultaneous contributions of linoleic and oleic acids, consequently no differentiation in terms of parent fatty acid was possible. On the contrary, the presence of hexanoic acid can mainly be attributable to the oxidative degradation of linoleic acid (the most abundant specie in LLL oxidation pattern), while octanoic, nonanoic, and decanoic acids were presumably derived from oleic acid (octanoic acid was the most abundant decay product in oxidized OOO, while no significant amounts of

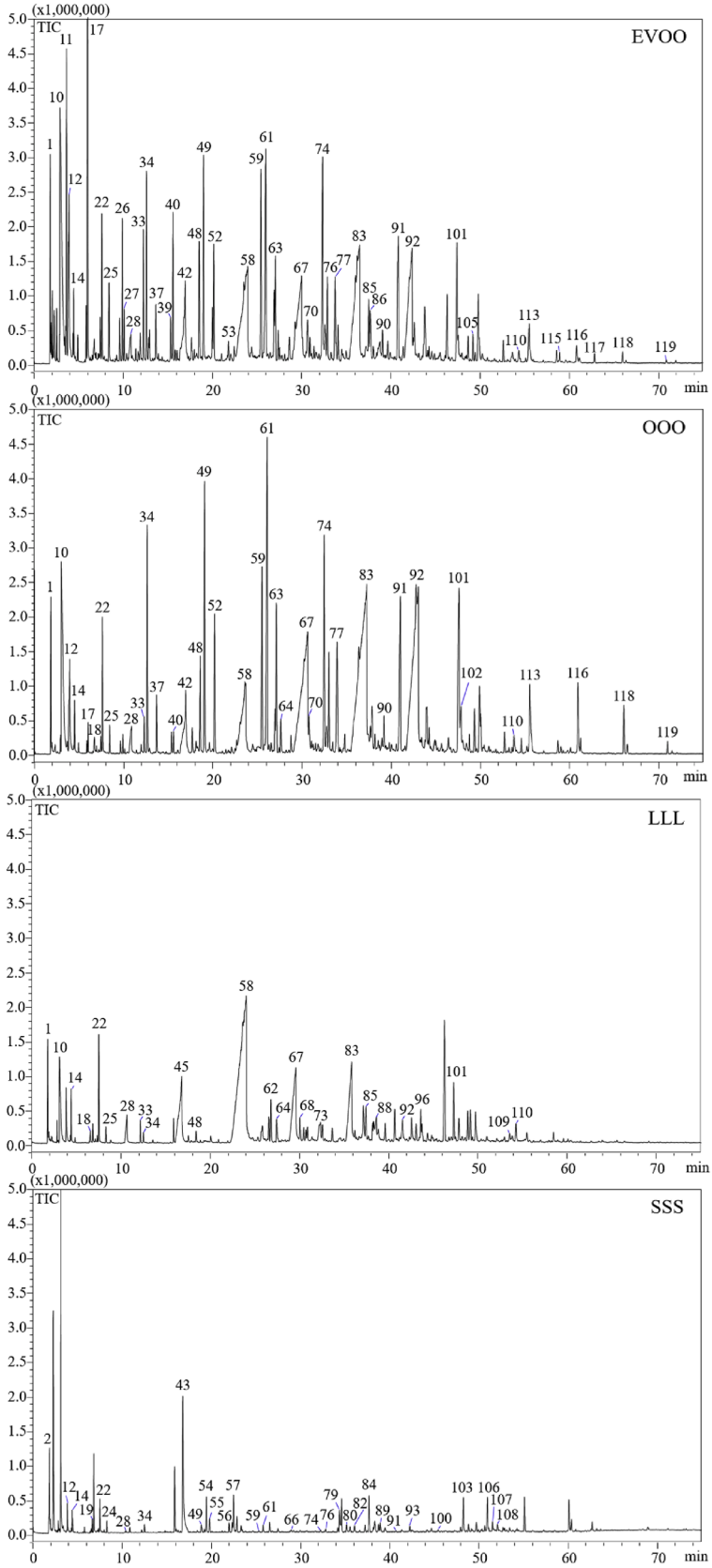

Fig. 3. HS-SPME-GC-MS chromatograms of secondary oxidation products in olive oil cultivar "biancolilla", OOO, LLL, and SSS oxidized samples.

nonanoic and decanoic acids were registered in other isologue TAGs). Therefore, considering that lipid composition of the olive oils follows a specific trend characterized by high proportion of oleic acid (55.00–83.00%) and minor amount of linoleic acid (2.50 to 21.00%) [30], it follows that a fluctuating proportion of pentanoic, hexanoic, heptanoic, octanoic, nonanoic and decanoic acids should be found in organic residues from olive oil according with their main parent fatty acids. However, further insights will be discussed in the next section where an alternative analytical approach involving a silylation step was used for the analysis of fatty acids by GC–MS and GC-FID analyses. Finally, hydrocarbons (*n*-heptane 2.14%, *n*-octane 3.58%, 1-nonene 1.16%, and 1-decene 1.43%), aldehydes (pentanal 0.46%, hexanal 1.12%, heptanal 1.84%, octanal 2.37%, nonanal 3.02%, decanal 0.95%, and dec-(2E)-enal 0.81%), and ketones (hexan-2-one 0.32%, heptan-2-one 1.19%, octan-2-one 1.25%, nonan-2-one 2.42%, decan-2-one 2.82%, undecane-2-one 0.27%) were also revealed among the secondary products of oxidation along with minor amounts of lactones (7.44%), esters (6.97%), furans (1.01%), and alcohols (0.20%).

3.4. TMS derivatives by GC–MS and GC-FID

For a detailed elucidation of fatty acids distribution in the oxidized EVOO samples, lipid compounds were converted into TMS derivatives by using BSTFA as silylating reagent. Such a reaction involves the formation of a TMS ether group [-Si-$(CH_3)_3$] on the hydroxyl resulting in the conversion of carboxylic acids and monoglycerides into more volatile and less polar TMS derivatives. The use of dichloromethane allowed the extraction of the TMS derivatives and other soluble compounds such as esters. GC–MS chromatograms of the olive oil cultivar "biancolilla" and oxidized TAG standards (see Fig. 4) confirmed the presence of a multitude of oxidized species classified as saturated fatty acid (SFA), monounsaturated fatty acid (MUFA), saturated fatty dicarboxylic acid (SFDA), esters of saturated fatty acids (ESFA), esters of monounsaturated fatty acids (EMUFA), and monoglycerides (MAGs). The list of the compounds identified in the analyzed samples is reported in Table 4.

Principal component analysis performed on the quantitative data obtained by GC-FID analyses (data reported in Table S.3) showed that distinctive regional patterns seen in olive oils before thermal treatment were no longer discernible in the oxidized samples. This loss of "regional specificity" was due to the formation of degradation products, and interestingly, this behavior was found to be independent of the olive oil origin. This trend is depicted in Fig. 5-A and 5-B through score and loading plots. In this context, PC1 can be interpreted as representing the degradation pathway of oleic acid, whereas PC2 appeared to reflect the degradation pathway of linoleic acid.

Despite the loading plot in Fig. 5-B, color-coding was used to group degradation products by their chemical nature, additional sub-loading plots were created to further explore the relationships among these compounds. These sub-loading plots, reported in Fig. 6-A/F, focus on specific classes of molecules, including MUFA, SFA, SFDA, ESFA, EMUFA, and MAGs. The distribution of MUFAs is depicted in Fig. 6-A, where it was evident that they were primarily distributed along PC1, where intact oleic (C18:1n9), *cis*-vaccenic (C18:1n7), and palmitoleic (C16:1n7) acids exhibited negative values on PC1, while their degradation products, specifically nonenoic (C9:1), decenoic (C10:1), and undecenoic (C11:1), were associated with positive values on PC1. This distribution suggested that PC1 mainly accounted for the degradation pathway of the oleic acid. Additionally, octenoic (C8:1n6) and heptenoic (C7:1) acids, featured by significant values on PC2, were likely formed as degradation products of the corresponding ω6 fatty acids, such as linoleic acid. In this case, the intact parent compound was not identified as the result of complete oxidation, but these results indicated that PC2 explained the degradation route of the linoleic acid.

Regarding SFAs as shown in Fig. 6-B, PC1 was featured by the presence of nonanoic (C9:0) and decanoic (C10:0) acids at positive values, along with intact palmitic (C16:0) and stearic (C18:0) acids at negative values. Other SFAs such as pentanoic (C5:0), hexanoic (C6:0), and heptanoic (C7:0) acids had a component only on PC2, whereas octanoic (C8:0) appeared on both on PC1 and PC2. According to general oxidation mechanisms and to what was discussed previously about MUFA, it was reasonable to assume that molecules with a significant component on PC1 were derived from the oxidation of the oleic acid, mainly C8:0, C9:0, and C10:0. Those with importance on PC2 as C6:0 were assigned to the oxidation of other unsaturated fatty acids such as linoleic acid and, to a lesser extent, *cis*-vaccenic acid. Such findings were like those previously illustrated in the section dedicated to the analysis of volatiles by means of HS-SPME-GC–MS and GC-FID technique. Among the mentioned SFAs, nonanoic acid was relatively the most abundant (with an average value of 8.31% across all samples), followed by octanoic acid (4.98%). The others were present in smaller amounts, with pentanoic, hexanoic, heptanoic, and decanoic acids at 0.62%, 1.57%, 1.84%, and 1.53%, respectively. This indicates that octanoic and nonanoic acids were the main degradation products and, therefore, likely originate from oleic acid which is the most abundant fatty acid in olive oil. The other SFAs were formed to a lower extent because they stem from less abundant unsaturated fatty acids or from less favored oxidation routes. Also, in Table 5 the correlation coefficients obtained plotting the relative concentration of each SFAs in relation to nonanoic and oleic acids are presented. Notably, nonanoic and decanoic acids were strongly correlated with oleic acid ($R^2 = 0.76$) and with each other ($R^2 = 0.90$). On the other hand, pentanoic and hexanoic were totally uncorrelated with both nonanoic and oleic acid. Unfortunately, it was not possible to examine the correlation with linoleic acid since it was not detected in the aged samples.

Such conclusions were supported by the degradation experiments conducted on standards of OOO, LLL and SSS triglycerides. Specifically, in the adopted experimental conditions, the carboxylic acids produced from the OOO oxidation were heptanoic, octanoic, nonanoic and decanoic acids. On the other hand, those generated from LLL included pentanoic, hexanoic, heptanoic, octanoic, and stearic acids. The loading plot of SFDAs in Fig. 6-C revealed the presence of only three dicarboxylic acids, namely succinic, suberic, and azelaic acids. The three acids were closely situated to each other and were positioned in the quadrant with positive values on PC1 and negative values on PC2. As per the discussion above regarding the interpretation of PCs, these dicarboxylic acids should be a product of the degradation route of oleic acid (evidenced by high values on PC1). However, they were on the opposite side compared to the other degradation products, namely pentanoic and hexanoic acids, which were associated with unsaturated fatty acids. Nevertheless, considering the degradation patterns of OOO and LLL standards, dicarboxylic acids were primarily generated from polyunsaturated fatty acids. In terms of relative concentrations succinic, suberic, and azelaic acids were featured by average values of 0.10%, 1.90% and 2.70%, respectively.

In Fig. 6-D the loading plot related to ESFAs is reported. The distribution of these esters reflected the carboxylic acid contents with the same number of carbon atoms, with a few exceptions. Carboxylic acids involved were octanoic, nonanoic, palmitic, and stearic acids, whereas the alcohols included propanol, butanol, pentanol, hexanol, heptanol, and octanol. Those having stearic and palmitic acid were predominantly distributed along PC2, consistent with the presence of SFAs shown in Fig. 6-B. Conversely, esters with octanoic and nonanoic acids had their main component on PC1, in agreement with the findings in Fig. 6-B. There was only one exception, which is octyl palmitate. It was positioned close to the octyl nonanoate, heptyl octanoate and heptyl nonanoate, and its formation was likely driven by octanol. Octanol is the initial oxidation product in the formation of the abundant octanoic acid, which could explain the unique distribution of octyl palmitate. The loading plot in Fig. 6-E illustrates the distribution of EMUFAs. Most of them were featured by the presence of oleic acid and as expected, they were positioned in the loading plot close to oleic acid (see Fig. 6-A). It is

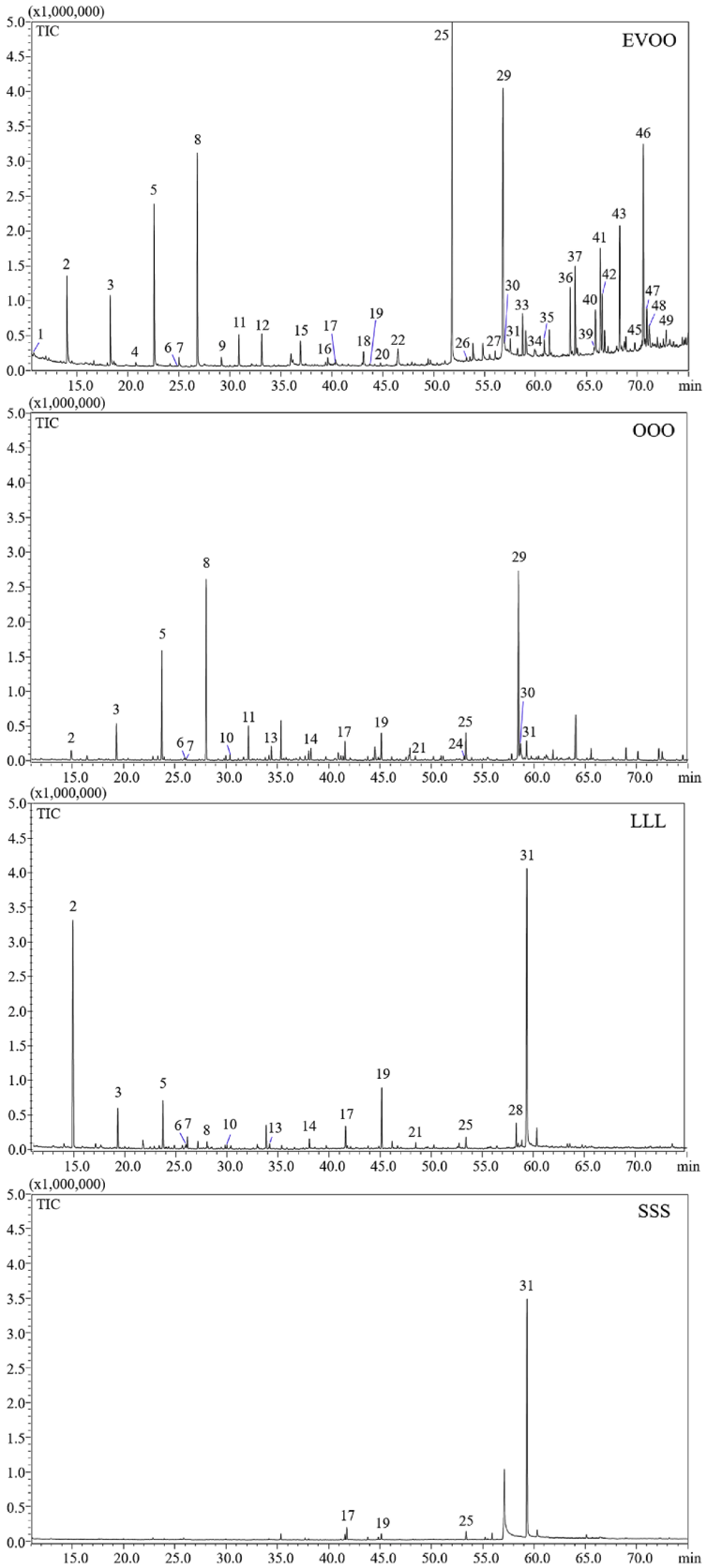

Fig. 4. GC–MS chromatograms of the olive oil cultivar "biancolilla", OOO, LLL, and SSS after the thermal oxidative process.

Table 4
List of compounds identified in EVOO "biancolilla" and TAGs after ageing process. Abbreviations: Class: chemical class; SFA: saturated fatty acid; MUFA: monounsaturated fatty acid; SFDA saturated fatty dicarboxylic acid; ESFA: esters of saturated fatty acids; EMUFA: esters of monounsaturated fatty acids; MAGs: monoglycerides; MS sim: mass spectral similarity; LRI_{exp}: experimental LRI; LRI_{ref}: reference LRI. As an example, the abundances (area%) of the EVOO cultivar "biancolilla" were reported.

ID	Common Name	Class	MS sim	LRI_{exp}	LRI_{ref}	EVOO
1	Pentanoic acid (TMS. C5:0)	SFA	90	980	974	0.58 ±0.02
2	Hexanoic acid (TMS. C6:0)	SFA	93	1072	1069	1.88 ±0.01
3	Heptanoic acid (TMS. C7:0)	SFA	93	1167	1166	1.39 ±0.00
4	Heptenoic acid (TMS. C7:1)	MUFA	90	1226	-	0.24 ±0.00
5	Octanoic acid (TMS. C8:0)	SFA	92	1262	1262	3.74 ±0.03
6	Succinic acid (2-TMS. C4:0)	SFDA	92	1312	1310	0.03 ±0.00
7	Octenoic acid C8:1n6)	MUFA	93	1316	-	0.43 ±0.01
8	Nonanoic acid (TMS. C9:0)	SFA	90	1359	1358	3.83 ±0.03
9	Nonenoic acid (TMS. C9:1)	MUFA	89	1418	-	0.35 ±0.00
10	Glutaric acid (2-TMS. C5:0)	SFDA	90	1404	1403	*nd*
11	Capric acid (TMS. C10:0)	SFA	90	1456	1456	0.72 ±0.01
12	Decenoic acid (TMS. C10:1)	MUFA	89	1515	-	0.92 ±0.03
13	Adipic acid (2-TMS. C6:0)	SFDA	90	1504	1503	*nd*
14	Pimelic acid (2-TMS. C7:0)	SFDA	90	1602	1601	*nd*
15	Undecenoic Acid (TMS. C11:1)	MUFA	91	1613	-	0.82 ±0.01
16	Heptyl octanoate	ESFA	91	1685	1680	0.24 ±0.01
17	Suberic acid (2-TMS. C8:0)	SFDA	90	1696	1694	0.59 ±0.07
18	Heptyl nonanoate	ESFA	90	1783	1779	0.25 ±0.00
19	Azelaic acid (2-TMS. C9:0)	SFDA	91	1795	1792	0.90 ±0.08
20	1-Monocaprylin (2-TMS. MAG-C8:0)	MAG	90	1831	-	0.15 ±0.00
21	Sebacic acid (2-TMS. C10:0)	SFDA	90	1891	1889	*nd*
22	Octyl nonanoate	ESFA	86	1882	1878	0.49 ±0.00
23	1-Mononanoin (2-TMS. MAG-C9:0)	MAG	89	1923	-	0.06 ±0.00
24	*cis*-Palmitoleic acid (TMS. C16:1n7)	MUFA	96	2023	2015	0.54 ±0.01
25	Palmitic acid (TMS. C16:0)	SFA	90	2045	2043	25.51 ±0.24
26	Propyl hexadecanoate	ESFA	89	2095	2077	0.07 ±0.00
27	Butyl hexadecanoate	ESFA	93	2191	2177	0.05 ±0.00
28	Linoleic acid (TMS. C18:2n6)	PUFA	96	2207	2205	*nd*
29	Oleic acid (TMS. C18:1n9)	MUFA	93	2215	2207	36.58 ±0.13
30	*cis*-Vaccenic Acid (TMS. C18:1n7)	MUFA	95	2222	2226	2.63 ±0.01
31	Stearic acid (TMS. C18:0)	SFA	93	2244	2237	5.09 ±0.01
32	Propyl octadecenoate	EMUFA	91	2269	2284	0.16 ±0.02
33	Pentyl hexadecenoate	EMUFA	96	2287	2276	0.69 ±0.04
34	Butyl octadecenoate	EMUFA	86	2330	-	0.25 ±0.00
35	Hexyl hexadecanoate	ESFA	90	2365	2375	0.26 ±0.00
36	Pentyl octadecenoate	EMUFA	92	1462	-	0.82 ±0.01
37	Heptyl hexadecanoate	ESFA	96	2481	2475	0.87 ±0.07
38	Pentyl octadecenoate	ESFA	91	2489	-	0.12 ±0.00
39	2-Monopalmitin (2-TMS. MAG-C16:0)	MAG	89	2553	-	0.08 ±0.00
40	Hexyl octadecenoate	EMUFA	92	2559	-	0.43 ±0.04
41	Octyl hexadecanoate	ESFA	94	2578	2574	0.86 ±0.01
42	1-Monopalmitin (2-TMS. MAG-C16:0)	MAG	93	2586	2581	0.59 ±0.01
43	Heptyl octadecenoate	EMUFA	93	2657	-	1.10 ±0.01
44	Heptyl octadecenoate	ESFA	93	2682	-	0.14 ±0.00
45	2-Monooleoin (2-TMS. MAG-C18:1n9)	MAG	89	2719	-	0.10 ±0.00
46	1-Monooleoin (2-TMS. MAG-C18:1n9)	MAG	89	2755	-	1.28 ±0.03
47	Octyl octadecenoate	EMUFA	86	2757	-	0.91 ±0.08
48	Octyl octadecenoate	ESFA	86	2779	2773	0.38 ±0.00
49	Nonyl octadecenoate	EMUFA	86	2854	-	0.34 ±0.00

interesting to note that the nonyl ester of oleic acid was located on the opposite side compared to the others. In general, the relative amount of these esters was relatively low, with only three of them reaching 1%, namely heptyl hexadecanoate, octyl hexadecanoate, nonyl octadecenoate. Finally, the loading plot in Fig. 6-F pertains to MAGs. The presence of such molecules in the oxidized EVOOs suggested that the hydrolysis of fatty acids from glycerol followed their oxidation. In fact, there were MAGs containing intact fatty acids, such as oleic and palmitic, which were positioned similarly to their hydrolyzed counterparts. Additionally, MAGs containing oxidized fatty acids, namely octanoic and nonanoic acid were also observed. The presence of these MAGs further supported the hypothesis that octanoic and nonanoic acids were the primary degradation products. Notably, the latter MAGs were in the opposite direction of 2-monooleoin. The positioning of 1-monooleoin and 2-monooleoin also suggested that the latter was the most resistant to hydrolysis since it was very close to the hydrolyzed oleic acid. Also, MAGs were molecules formed in a relatively low percentage, with 1-monooleoin being the most abundant, with an average value of 0.87%. As a final consideration, the oxidation processes involving unsaturated fatty acids result in the generation of various secondary products of oxidation. These include mono-carboxylic and dicarboxylic acids with acyl chains ranging from five to ten atoms, encompassing mainly saturated forms. Additionally, a series of esters and MAGs were detected. Some of these potential archaeological biomarkers show a high degree of hydrophilicity, especially for dicarboxylic acids characterized by two carboxylic groups along their acyl chains. This limits their entrapment in organic and mineral residues due to humidity or rainwater in burial environments preventing their detection. In conclusion, the complete elucidation of the oxidized lipid species in olive oils and TAGs standards induced by in-lab thermal treatment at 120 °C in air for three weeks indicated that the mono-carboxylic acids as pentanoic, hexanoic, heptanoic, octanoic, nonanoic and decanoic acids can simultaneously be considered as probable archaeological biomarkers suggesting the presence of lipid substances coming from olive oil. However,

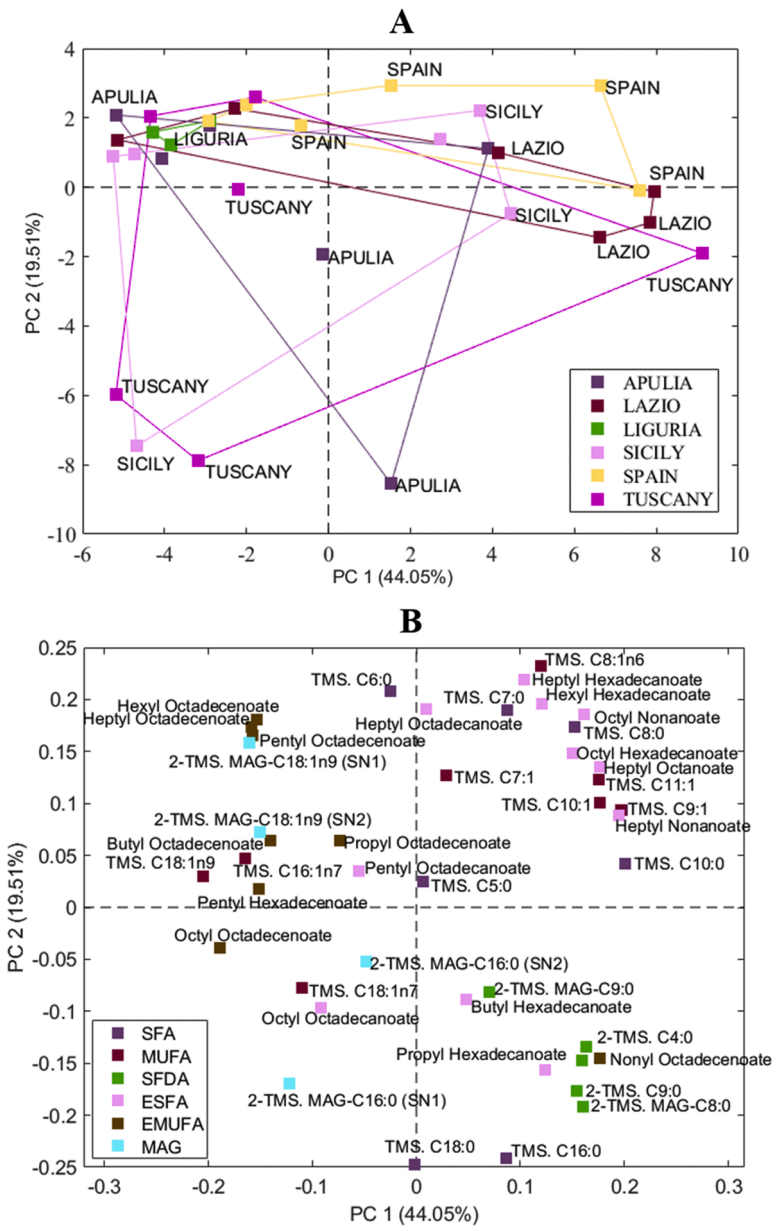

Fig. 5. Score (A) and loading (B) plots of the GC-FID data relative to the aged samples.

it must be emphasized that establishment of specific and selective fatty acid ratios indicative of olive oil origin may be challenging due to the widespread distribution of oleic and linoleic acids across plant kingdoms. This complexity further complicates interpretations regarding the origin of lipid matter. Therefore, it is crucial for analysts and archaeologists to collaborate closely to ensure a coherent attribution of lipid organic matter, aligned with the function of the ceramic vessels [2].

3.5. Archaeological insights

Lipid contents of twenty-four archaeological samples coming from the excavations of the area of *Villa San Pancrazio, Taormina*, were assessed by GC–MS. These samples were grouped in three different categories as follows: *amphorae* (10 samples), *unguentaria* (5 samples), and *lamps* (9 samples). All analyzed samples showed the presence of palmitic, stearic, and oleic acids as the main components, while no traces of the selected archaeological biomarkers were detected in the total ion current chromatogram (TIC). These preliminary results indicated a probable presence of organic lipid matter, but the ubiquitous nature of these molecules led the authors to carry out further investigations. Thus, the fragment ions specific for each target archaeological biomarker (pentanoic acid, 159 *m/z*; hexanoic acid, 173 *m/z*; heptanoic acid, 187 *m/z*; octanoic acid, 201 *m/z*; nonanoic acid, 215 *m/z*; decanoic acid, 229 *m/z*) were extracted and monitored. The obtained extracted ion chromatograms (EIC) of all pottery samples revealed the presence of the archaeological biomarkers at trace levels, independently from the function of artifact. This aspect is of fundamental importance since it confirms the hypothesis that porous ceramic matrix can preserve the lipid matter [2]. On the contrary, soil and encrustation samples showed a significant variability in this research study. For example, the only soil samples that showed the presence of all mono-carboxylic acids, from pentanoic to decanoic acids, were US3329 RO 11, US3329 RO 21, and US3329 RO 26, grouped in *amphora* category, while all other samples revealed only the presence of octanoic and nonanoic acids. Probably, this behavior may be related to the nature of the analyzed samples not particularly able to encapsule and preserve lipid residues.

As an example, the EIC of the sample *amphora* US3329 RO 25 is shown in Fig. 7. It should be noted an excessive amount of pentanoic

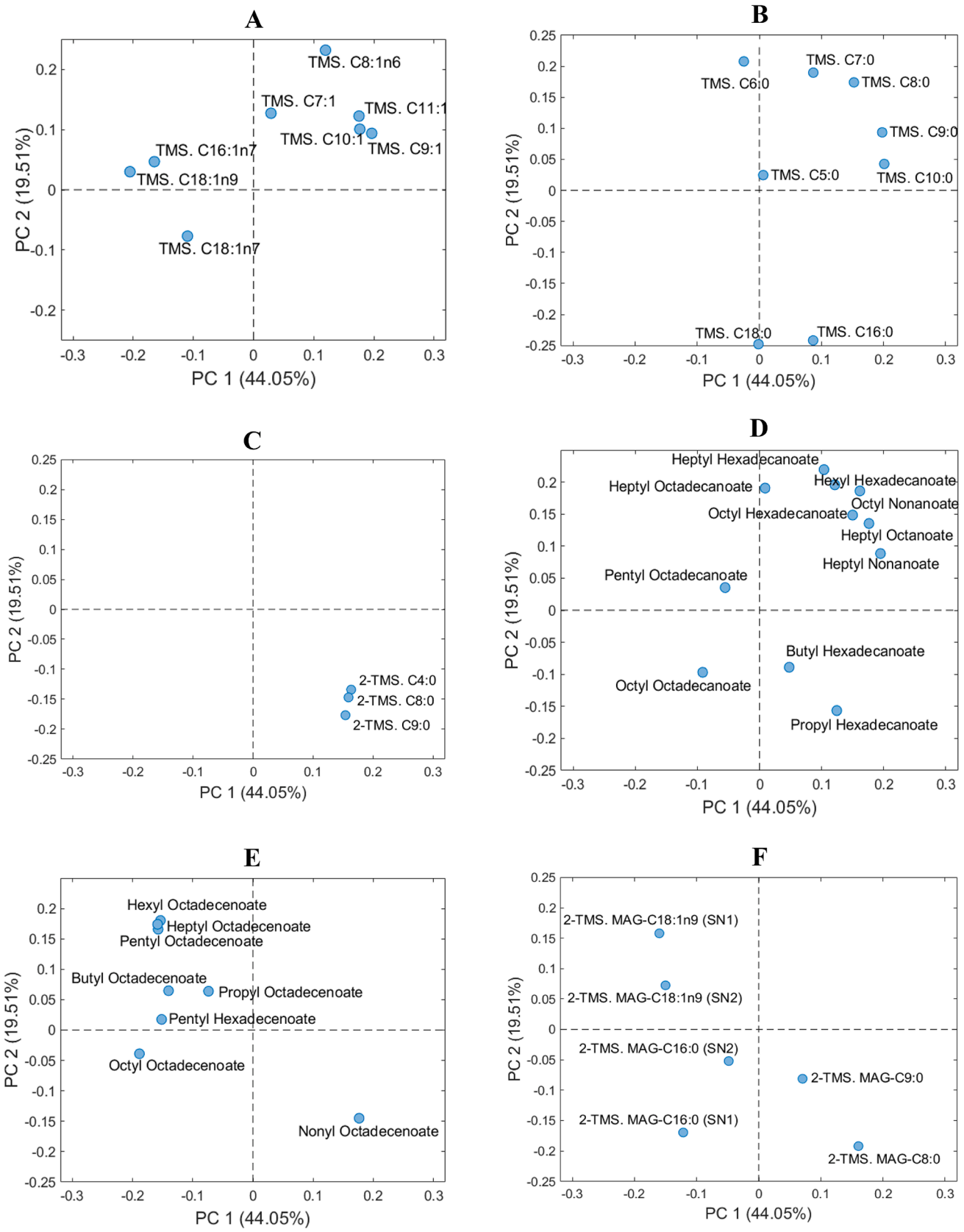

Fig. 6. Loading plots of the monounsaturated fatty acids (MUFA) (A), saturated fatty acids (SFA) (B), saturated fatty dicarboxylic acid (SFDA) (C), esters of saturated fatty acids (ESFA) (D), esters of monounsaturated fatty acids (EMUFA) (E), and monoacylglycerols (MAGs) (F).

Table 5
Correlation coefficients obtained from the regression of the relative concentration of SFAs with respect to nonanoic and oleic acid.

Mono-carboxylic acid	R^2 nonanoic acid	R^2 oleic acid
Pentanoic acid	0.005	0.010
Hexanoic acid	0.006	0.001
Heptanoic acid	0.340	0.200
Octanoic acid	0.770	0.480
Nonanoic acid	1.000	0.760
Decanoic acid	0.900	0.760
Octadecanoic acid	0.760	1.000

acid (pink trace in Fig. 7) not referable to the typical oxidized fingerprint of olive oil, suggesting the presence of lipid organic material probably coming from other sources, like a mixture of olive oil with animal bones and charred elements, possibly used for preserving animal meat or for the preparation of *medicamenta*. In literary sources, in fact, there is evidence of the use of olive oil mixed with calf fat, dry and liquid pine pitch, beeswax and other ingredients to create a poultice used in the treatment of fractures, called Moschione's remedy [31]. Nevertheless, these findings implied that investigated *amphorae* (Spinella type and Keay LII type), may have contained vegetable lipid material such as olive oil, according to mono-carboxylic acids profiles observed in the pottery samples of such category. This information is extremely interesting considering that these *amphorae* have so far been solely associated with the storage of wine.

With respect to *unguentarium* category, 2052–1 sample (pottery) was the only archaeological find to reveal the presence of all the mono-carboxylic acids designed as archaeological biomarkers, indicating the degradation of a vegetable oil, likely olive oil, in accordance with the function of the *unguentarium* in ancient times.

Finally, regarding the *lamp* category, only soil samples were analyzed, and the EIC revealed the presence of octanoic and nonanoic acids at trace levels, as previously described. Therefore, it was not possible to establish the nature of the lipid matter.

4. Conclusions

This work provides a comprehensive characterization of the degradation products resulting from in-lab thermal oxidative treatments carried out on extra-virgin olive oils, with the ultimate goal of identifying specific archaeological biomarkers for olive oil. Various analytical techniques have been useful in this regard and the application of chemometric tools on the acquired data was crucial for their interpretation. PCA on quantitative GC-FID data revealed that distinctive regional patterns observed before thermal treatment were no longer discernible in the oxidized samples. The complete elucidation of the oxidized lipid species in aged olive oils indicated the mono-carboxylic acids, such as pentanoic, hexanoic, heptanoic, octanoic, nonanoic, and decanoic acids as probable archaeological biomarkers useful for indicating the presence of lipid substances coming from olive oil in archaeological organic residues. Such conclusions were supported by the degradation experiments conducted on standards of OOO, LLL and SSS triglycerides. However, it must be emphasized that the establishment of specific and selective fatty acids fingerprint indicative of olive oil still remains challenging due to the ubiquitous distribution of oleic and linoleic acids in plant kingdoms, thus complicating interpretations of lipid matter origins. Therefore, the strict collaboration between analysts and archaeologists is crucial to ensure coherent attribution of the lipid organic matter, in accordance with the function of the original ceramic vessel.

Finally, the lipid contents of twenty-four samples grouped in *amphorae, unguentaria,* and *lamps* categories, coming from the excavations of the *Villa San Pancrazio* area in *Taormina*, were determined. The analytical results obtained on the *amphorae* (Spinella type and Keay LII type) samples revealed the presence of mono-carboxylic acids referable to lipid oxidation of olive oils, an information extremely interesting considering that this type of *amphorae* have so far been solely associated with the storage of wine.

Funding

The research was conducted within the PON Research and Innovation 2014–2020 project funded by Italian Ministry of University and Research (MUR).

CRediT authorship contribution statement

Valentina Chiaia: Visualization, Formal analysis, Data curation. **Giuseppe Micalizzi:** Writing – review & editing, Writing – original draft, Supervision, Investigation, Data curation, Conceptualization. **Danilo Donnarumma:** Writing – review & editing, Writing – original draft, Formal analysis, Data curation. **Anna Irto:** Formal analysis, Data curation, Conceptualization. **Clemente Bretti:** Visualization, Investigation, Formal analysis, Data curation. **Marta Venuti:** Writing – original draft, Investigation, Conceptualization. **Gabriele Lando:** Writing –

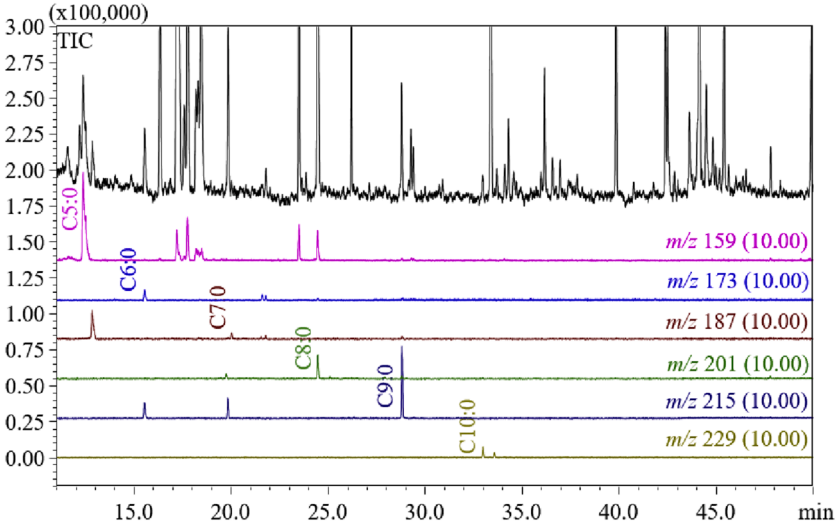

Fig. 7. EIC chromatogram of the lipid extract from the *amphorae* sample (sample cod. US3329 RO 25). Selected fragment ions: pentanoic acid, 159 *m/z*; hexanoic acid, 173 *m/z*; heptanoic acid, 187 *m/z*; octanoic acid, 201 *m/z*; nonanoic acid, 215 *m/z*; decanoic acid, 229 *m/z*.

review & editing, Writing – original draft, Software, Investigation, Conceptualization. **Luigi Mondello:** Writing – review & editing, Writing – original draft, Visualization, Supervision, Conceptualization. **Paola Cardiano:** Writing – review & editing, Writing – original draft, Visualization, Validation, Supervision, Project administration, Conceptualization.

Declaration of competing interest

The authors declare that they have no known competing financial interests or personal relationships that could have appeared to influence the work reported in this paper.

Data availability

The authors are unable or have chosen not to specify which data has been used.

Acknowledgments

The Authors thank Merck Life Science and Shimadzu Corporations for their continuous support; we extend our gratitude to the Superintendence of Cultural Heritage of Messina for their demonstrated liberality.

Supplementary materials

Supplementary material associated with this article can be found, in the online version, at doi:10.1016/j.chroma.2024.465154.

References

[1] R.P. Evershed, Biomolecular archaeology and lipids, World Archaeol. 25 (1) (1993) 74–93, https://doi.org/10.1080/00438243.1993.9980229.
[2] A. Irto, G. Micalizzi, C. Bretti, V. Chiaia, L. Mondello, P. Cardiano, Lipids in Archaeological Pottery: a Review on Their Sampling and Extraction Techniques, Molecules. 27 (11) (2022), https://doi.org/10.3390/molecules27113451.
[3] M.K. Jones, D.E.G. Briggs, G. Eglington, E. Hagelberg, R.P. Evershed, S.N. Dudd, S. Charters, H. Mottram, A.W. Stott, A. Raven, P.F. van Bergen, H.A. Bland, Lipids as carriers of anthropogenic signals from prehistory, Philosophical Trans. R. Soc. London. Series B: Biol. Sci. 354 (1379) (1999) 19–31, https://doi.org/10.1098/rstb.1999.0357.
[4] C. Heron, R.P. Evershed, The analysis of organic residues and the study of pottery use, Archaeol. Method Theory 5 (1993) 247–284.
[5] M. Regert, Analytical strategies for discriminating archeological fatty substances from animal origin, Mass Spectrom. Rev. 30 (2) (2011) 177–220, https://doi.org/10.1002/mas.20271.
[6] M.S. Copley, H.A. Bland, P. Rose, M. Horton, R.P. Evershed, Gas chromatographic, mass spectrometric and stable carbon isotopic investigations of organic residues of plant oils and animal fats employed as illuminants in archaeological lamps from Egypt, Analyst 130 (6) (2005) 860–871, https://doi.org/10.1039/B500403A.
[7] T.F.M. Oudemans, J.J. Boon, Molecular archaeology: analysis of charred (food) remains from prehistoric pottery by pyrolysis—Gas chromatography/mass spectrometry, J. Anal. Appl. Pyrolysis. 20 (1991) 197–227, https://doi.org/10.1016/0165-2370(91)80073-H.
[8] J. Dunne, A. Chapman, P. Blinkhorn, R.P. Evershed, Fit for purpose? Organic residue analysis and vessel specialisation: the perfectly utilitarian medieval pottery assemblage from West Cotton, Raunds, J. Archaeol. Sci. 120 (2020) 105178, https://doi.org/10.1016/j.jas.2020.105178.
[9] M. Bondetti, E. Scott, B. Courel, A. Lucquin, S. Shoda, J. Lundy, C. Labra-Odde, L. Drieu, O.E. Craig, Investigating the formation and diagnostic value of ω-(o-alkylphenyl)alkanoic acids in ancient pottery, Archaeometry. 63 (3) (2021) 594–608, https://doi.org/10.1111/arcm.12631.
[10] M.P. Colombini, F. Modugno, E. Ribechini, Organic mass spectrometry in archaeology: evidence for Brassicaceae seed oil in Egyptian ceramic lamps, J. Mass Spectrometry 40 (7) (2005) 890–898, https://doi.org/10.1002/jms.865.
[11] I. Ferro, L'anfora di tipo Keay LII: indicatore archeologico nel Mediterraneo tardo-antico., Givigliano (2006). In Calabria… riflessi di una storia "minore" al centro del Mediterraneo Edizioni Scientifiche Italiane, Napoli (2006).
[12] A. Ollà, La produzione di anfore vinarie a Naxos (III aC-V dC), Naxos di Sicilia in età romana e bizantina ed evidenze dai Peloritani. Catalogo Mostra Archeologica Museo di Naxos (3 dicembre 1999-3 gennaio 2000), Bari, (2001) 47–60.
[13] M. Miano, Tra Naxos e Tauromenion: dinamiche insediative nella valle del fiume Alcantara, 2021.
[14] M. Oteri, F. Rigano, G. Micalizzi, M. Casale, C. Malegori, P. Dugo, L. Mondello, Comparison of lipid profile of Italian Extra Virgin Olive Oils by using rapid chromatographic approaches, J. Food Comp. Anal. 110 (2022) 104531, https://doi.org/10.1016/j.jfca.2022.104531.
[15] F. Rigano, M. Oteri, G. Micalizzi, D. Mangraviti, P. Dugo, L. Mondello, Lipid profile of fish species by liquid chromatography coupled to mass spectrometry and a novel linear retention index database, J. Sep. Sci. 43 (9–10) (2020) 1773–1780, https://doi.org/10.1002/jssc.202000171.
[16] V.D. Zheljazkov, G. Micalizzi, S. Yilma, C.L. Cantrell, A. Reichley, L. Mondello, I. Semerdjieva, T. Radoukova, Melissa officinalis L. as a Sprout Suppressor in Solanum tuberosum L. and an Alternative to Synthetic Pesticides, J. Agric. Food Chem. 70 (44) (2022) 14205–14219, https://doi.org/10.1021/acs.jafc.2c05942.
[17] L. Campagna, A. Toscano Raffa, M. Venuti, M.C. Papale, M. Miano, Lo scavo nella Villa San Pancrazio a Taormina : relazione preliminare sulle attività delle campagne 2015-2017, (2017). https://doi.org/10.19272/201711301006.
[18] M. Venuti, Taormina: trasformazioni del paesaggio urbano tra Tarda antichità e Medioevo, Quasar.2022.
[19] O. Gomez-Laserna, A. Irto, P. Irizar, G. Lando, C. Bretti, I. Martinez-Arkarazo, L. Campagna, P. Cardian, o, Non-Invasive Approach to Investigate the Mineralogy and Production Technology of the Mosaic Tesserae from the Roman Domus of Villa San Pancrazio (Taormina, Italy), Crystals 11 11 (2021), https://doi.org/10.3390/cryst11111423.
[20] A. Pecci, E. Degl'Innocenti, G. Giorgi, M.Á.Cau Ontiveros, F. Cantini, E. Solanes Potrony, C. Alós, D. Miriello, Organic residue analysis of experimental, medieval, and post-medieval glazed ceramics, Archaeol. Anthropol. Sci. 8 (4) (2016) 879–890, https://doi.org/10.1007/s12520-015-0262-3.
[21] L. Cerretani, A. Bendini, A.D. Caro, A. Piga, V. Vacca, M.F. Caboni, T. Gallina Toschi, Preliminary characterisation of virgin olive oils obtained from different cultivars in Sardinia, Eur. Food Res. Technol. 222 (3) (2006) 354–361, https://doi.org/10.1007/s00217-005-0088-9.
[22] M. D'Imperio, G. Dugo, M. Alfa, L. Mannina, A.L. Segre, Statistical analysis on Sicilian olive oils, Food Chem. 102 (3) (2007) 956–965, https://doi.org/10.1016/j.foodchem.2006.03.003.
[23] G. Paquette, D.B. Kupranycz, F.R. van de Voort, The mechanisms of lipid autoxidation I. Primary oxidation products, Can. Inst. Food Sci. Technol. J. 18 (2) (1985) 112–118, https://doi.org/10.1016/S0315-5463(85)71767-1.
[24] L. Xu, X. Yu, M. Li, J. Chen, X. Wang, Monitoring oxidative stability and changes in key volatile compounds in edible oils during ambient storage through HS-SPME/GC–MS, Int. J. Food Properties 20 (sup3) (2017) S2926–S2938, https://doi.org/10.1080/10942912.2017.1382510.
[25] E. Selke, W.K. Rohwedder, H.J. Dutton, Volatile components from tristearin heated in air, J. Am. Oil. Chem. Soc. 52 (7) (1975) 232–235, https://doi.org/10.1007/BF02639148.
[26] D.R. Nelson, D.R. Sukkestad, R.G. Zaylskie, Mass spectra of methyl-branched hydrocarbons from eggs of the tobacco hornworm, J. Lipid Res. 13 (3) (1972) 413–421, https://doi.org/10.1016/S0022-2275(20)39405-0.
[27] E. Selke, W.K. Rohwedder, H.J. Dutton, Volatile components from trilinolein heated in air, J. Am. Oil. Chem. Soc. 57 (1) (1980) 25–30, https://doi.org/10.1007/BF02675520.
[28] K. Watanabe, Y. Sato, Lactones produced through thermal oxidation of higher fatty acids, Agric. Biol. Chem. 35 (2) (1971) 278–281, https://doi.org/10.1080/00021369.1971.10859912.
[29] S. Grebenteuch, C. Kanzler, S. Klaußnitzer, L.W. Kroh, S. Rohn, The Formation of Methyl Ketones during Lipid Oxidation at Elevated Temperatures, Molecules. 26 (4) (2021), https://doi.org/10.3390/molecules26041104.
[30] P.K. Revelou, M. Xagoraris, A. Alexandropoulou, C.D. Kanakis, G.K. Papadopoulos, C.S. Pappas, P.A. Tarantilis, Chemometric Study of Fatty Acid Composition of Virgin Olive Oil from Four Widespread Greek Cultivars, Molecules. 26 (14) (2021), https://doi.org/10.3390/molecules26144151.
[31] G. Semeraro, M.V. Aquilino, Balsami e unguenti nei Late Roman unguentaria da Hierapolis di Frigia (Turchia): studio archeologico e analisi chimica dei contenuti, Studi classici e orientali : LXVII, tomo II, 2021, Pisa (2021) 353–373, https://doi.org/10.12871/978883339626220.